# Numerical Simulation Analysis of Construction Support of Intersection Section in Extra-long Water Diversion Project Tunnels

Juan Li[1,a], Jianwen Zhu[1,b], Fei Ma[1,c], Kezhong Wang[2,d]

[1] Wanjiazhai Water Control Holding Group Co., Ltd.

[2] College of Civil Engineering，Zhejiang University of Technology.

[a] 459680874@qq.com, [b] 351471245@qq.com, [c] 582245893@qq.com, [d]wkjtjybyy@126.com

**Abstract.** The selected Middle Yellow River Diversion Project is an important backbone project of the planning and construction of the modern water network in Shanxi Province. The project is composed of water source project and water transmission project, the water transmission project is about 400 kilometers long, there are about 200 kilometers of total dry, about 100 kilometers of East Dry and West Dry each, with an average depth of about 400 meters. The intersection section studied in this paper is located under the ridgeline of Lvliang Mountain with a burial depth of more than 600 meters. Whether to support the excavation of the tunnel intersection section was simulated by three-dimensional numerical simulation analysis of different sections. The stress field of surrounding rock and liner and the distribution of plastic zones in surrounding rock were simulated and calculated. The research results provide a technical reference for the design of tunnel support and the formulation of construction schemes, which is of great significance for the construction safety and operation management of water diversion tunnels.

**Keywords:** Super long tunnel; intersection section; support; numerical simulation.

## 1. Introduction

To solve the problem of unbalanced water resources, an important method is to diversion and transfer water. Due to the limitations of topography and landform of water source areas and water diversion lines, the construction of deep buried and extra-long water diversion tunnels will increasingly be used [1-2]. For high buried depth tunnels, affected by the ground stress and the condition of surrounding rock, the tunnel intersection section is a high-risk area for tunnel engineering construction and also a key monitoring location for later operation and management. Therefore, it is of great engineering significance to study the support of tunnel intersection section in depth [3-4]. Three-dimensional numerical analysis can simulate the process of tunnel excavation and support well [5-6], while factors such as the excavation unloading effect of tunnel [7], the timing of rock mass excavation and support [8-9], the change of stress in surrounding rock and the loosening of surrounding rock [10-11], etc., have a great influence on numerical simulation analysis. Therefore, the study of three-dimensional numerical simulation analysis considering the excavation unloading effect is of great significance for the safety evaluation and design optimization of underground water diversion tunnel engineering construction [12].

## 2. Project overview

The Middle Yellow River Diversion Project is a large-scale backbone water diversion project with the longest water transmission line, the most widely covered counties and cities, the largest investment scale and the most benefited population in the construction of modern water network in Shanxi Province. It is planned to supply 305 million cubic meters of water annually. The 12# construction access adit intersects with the 2# Xiangfling branch tunnel at the K47+476.87 stake. The total length of the 12# construction access adit is 450 m, with a longitudinal gradient of -10.2% (5.824° angle of inclination), parallel to the main hole (the 2# Xiangfling branch tunnel), with a horizontal spacing of 103.7 m, and finally intersecting at 44° with a 136° angle. The Xiangfling 2#

hole at the intersection is about 65 m buried depth, the surrounding rock is IV type, mainly limestone and mudstone, with a small amount of water leakage, strong weathering, and a small amount of clay inclusion. After excavation, it is prone to block falling.

## 3. Calculation methods and models

### 3.1 Analysis theory

The support parameters shown in Table 1 were used in the calculation process. The ground stress field is mainly composed of self-weight stress, and the side pressure coefficient is assumed to be 0.6-0.8 according to engineering experience. The surrounding rock is considered as elastoplastic material, and the Mohr-Coulomb model is adopted for the constitutive model; the sprayed concrete and the slab concrete are modeled by solid element models. An elastic model is adopted; the support effect of the steel arch frame is equivalent to the spray concrete by the equivalent method, and the calculation formula is as follows：

$$\mathrm{E} = E_0 + \frac{S_g \times E_g}{S_c} \qquad (1)$$

Where, $E$ is the elastic modulus of the equivalent concrete primary lining structure after conversion; $E_0$ is the elastic modulus of the original concrete; $S_g$ is the cross-sectional area of the steel arch frame; $S_c$ is the cross-sectional area of the concrete; and $E_g$ is the elastic modulus of the steel.

Table 1 Mechanical Parameters for Calculation

| Surrounding rock categories | Density D(kg/m$^3$) | Elastic modulus E(GPa) | Poisson's ratio μ | Cohesion C（MPa） | Angle of internal friction φ（°） |
|---|---|---|---|---|---|
| Limestone (IV type) | 2700 | 1.5 | 0.35 | 0.15 | 27 |
| Sprayed concrete C20 | 2400 | 25.5 | 0.20 | / | / |
| Slab concrete C25 | 2400 | 28 | 0.20 | / | / |
| Steel arch frame | 7850 | 200 | 0.3 | / | / |

### 3.2 Numerical model

This calculation uses Unigraphics NX to model the three-dimensional solid, divides the grid through ANSYS software, and finally performs the numerical simulation analysis using the finite difference program FLAC3D. A three-dimensional model is established as shown in Fig 1, with the center of the bottom slab of the 2# hole of the Jiaofenling branch line at the intersection of the two tunnel axes as the origin, and the axis direction of the 2# hole of the Jiaofenling branch line as the x-axis direction, 60 m in length; the positive direction of the z-axis is vertically upward, and 15 m is taken downward from the origin and 20 m upward; the y-axis direction is 36 m in total. The overall grid division is shown in Fig 2, with a total of 134,500 elements and 261,500 nodes. A vertical section along the axis of the 2# hole of the Jiaofenling branch line is selected, with the coordinate position x = 0 m, as section 1-1; a vertical section along the axis of the 12# construction adit is selected, as section 2-2; a section at the intersection of the two tunnel axes perpendicular to the axis of the 2# hole of the Jiaofenling branch line is selected, with the coordinate position x = 0 m, as section 3-3.

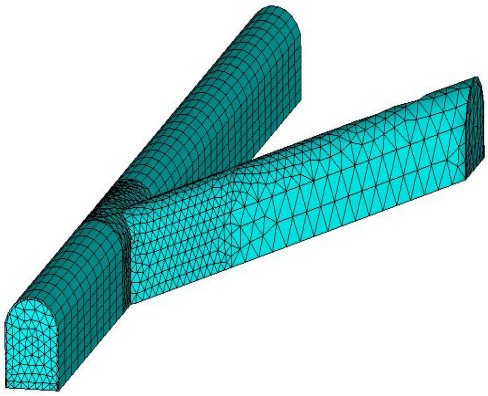

Fig 1 Three-dimensional model diagram

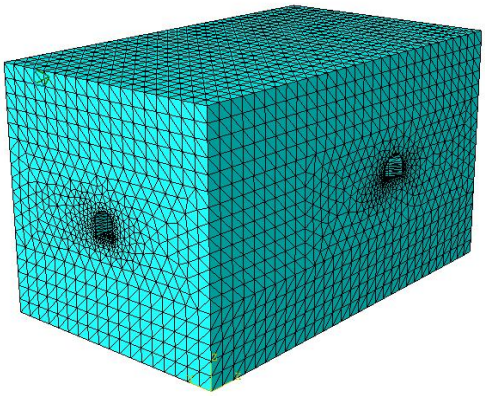

Fig 2 Overall grid division of the model

## 4. Computational analysis

The construction section of the tunnel section of this project is a city gate shape, with a designed water depth of 2.2 to 2.5 meters. The 12# branch tunnel is a construction branch tunnel, and the 2# hole of the Fuliang branch line is a water diversion tunnel. The 12# construction branch tunnel is excavated first, and then the 2# hole of the Fuliang branch line is excavated simultaneously on both sides. The shape of the tunnel section is a city gate shape, and the support form is a combined support of "steel arch frame +mesh + anchor rod + shotcrete". In category IV surrounding rock, the thickness of shotcrete in the 2# hole of the Fuliang branch line is 100mm, and I14 I-beam steel arch frames are used. The longitudinal spacing of steel arch frames and system anchor bars is 1.2m; the thickness of shotcrete in the 12# construction branch tunnel is 210~270mm. The process of tunnel excavation is also a process in which the stress of surrounding rock is released and redistributed. Whether support is given has a great impact on the three-dimensional elastoplastic simulation analysis of tunnel construction. The following are two different cases whether considering the effect of excavation unloading, simulate the stress field of tunnel surrounding rock and the distribution of surrounding rock plastic zone, etc., and analyze the stability of tunnel surrounding rock and lining structure. Select three typical sections 1-1, 2-2, 3-3 for analysis and research.

### 4.1 Structural stability analysis without support after excavation

Section 1-1 (the axis of the Fuliang branch line 2# tunnel) is selected for analysis. The vertical displacement of the cross-section along the axis of the Fuliang branch line 2# tunnel increases near the intersection of the two tunnels. The value of the crown settlement away from the intersection is about 6mm (↓), and the value of the bottom plate uplift is about 5mm (↑). At the intersection of the two tunnels, the maximum value of the crown settlement is 9.6mm (↑), and the maximum value of the bottom plate uplift is 7.4mm (↓). The range of displacement increase is about 10m on the obtuse side of the intersection and about 16m on the acute side of the intersection, as shown in Fig 3.Section 2-2 along the axis of the construction gallery 12# is a vertical section. The maximum values of the crown settlement and bottom plate uplift of the construction gallery 12# occur at the intersection with the Fuliang branch line 2# hole, with the maximum value of the crown settlement being 10.8mm (↓) and the maximum value of the bottom plate uplift being 7.6mm (↑). The deformation of the surrounding rock in the range of 14m from the intersection point in the construction gallery 12# is greatly affected by the intersection. Fig 4 shows this.

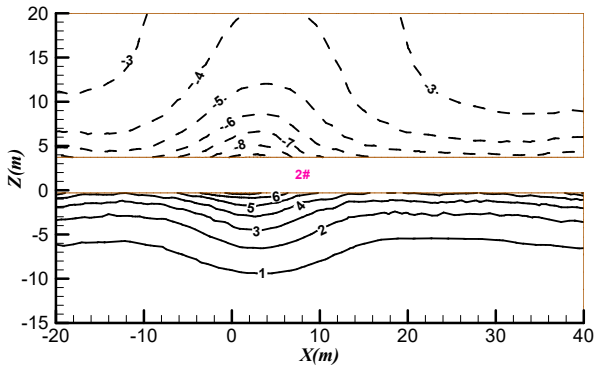


Fig 3 Section 1-1 vertical displacement contour

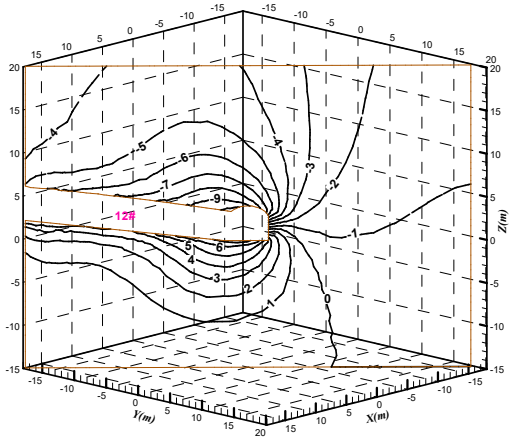


Fig 4 Section 2-2 vertical displacement contour

Section 3-3 is located at the intersection of the axes of the two tunnels and perpendicular to the axis of the Fuliang branch line 2# tunnel. The maximum value of settlement is 10.2mm (↓), which occurs at the intersection of the linings of the two tunnels at the top, and the maximum value of the bottom plate uplift is 7.5mm (↑). The lining of the two tunnels at the top intersection appears as a "sharp angle", and the rock blocks at the sharp angle are unstable and prone to block dropout, as shown in Fig 5（a）. The maximum value of the horizontal displacement at the middle of the left side wall of the construction gallery 12# is 6.7mm; the maximum value of the horizontal displacement at the middle of the right side wall of the Fuliang branch line 2# tunnel is -7.5mm, as shown in Fig 5(b).

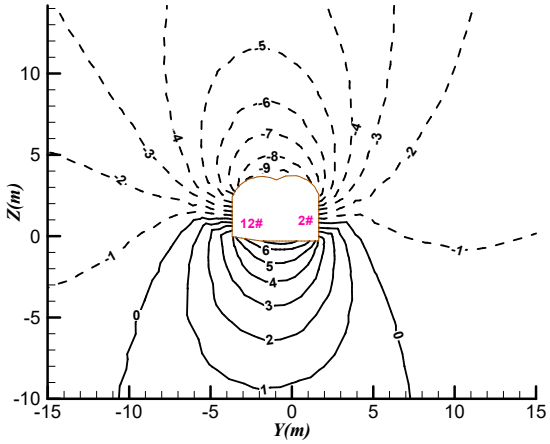


Vertical displacement contour

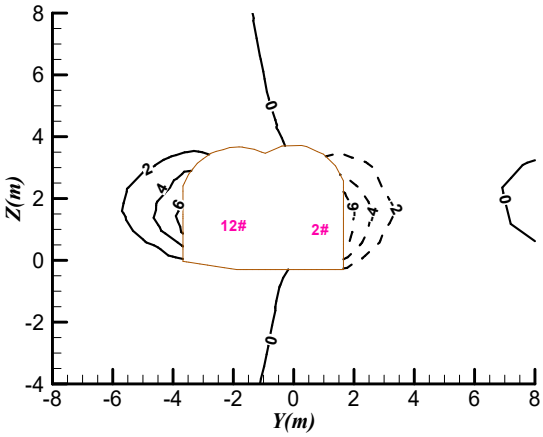


b. Horizontal displacement contour

Fig 5 Section 3-3 vertical and horizontal displacement contours

The rock compression stress at the bottom of the construction gallery 12# near the left wall foot is relatively large, at 4.07 MPa; the compression stress at the right side of the arch waist of the Fuliang branch line 2# tunnel is relatively large, at 3.0 MPa, and the maximum principal stress is shown in Fig 6(a).A small tension region is observed in the middle of the right side wall of the Fuliang branch line 2# tunnel, with a maximum value of 0.097 MPa, and the minimum principal stress is shown in Fig 6(b).

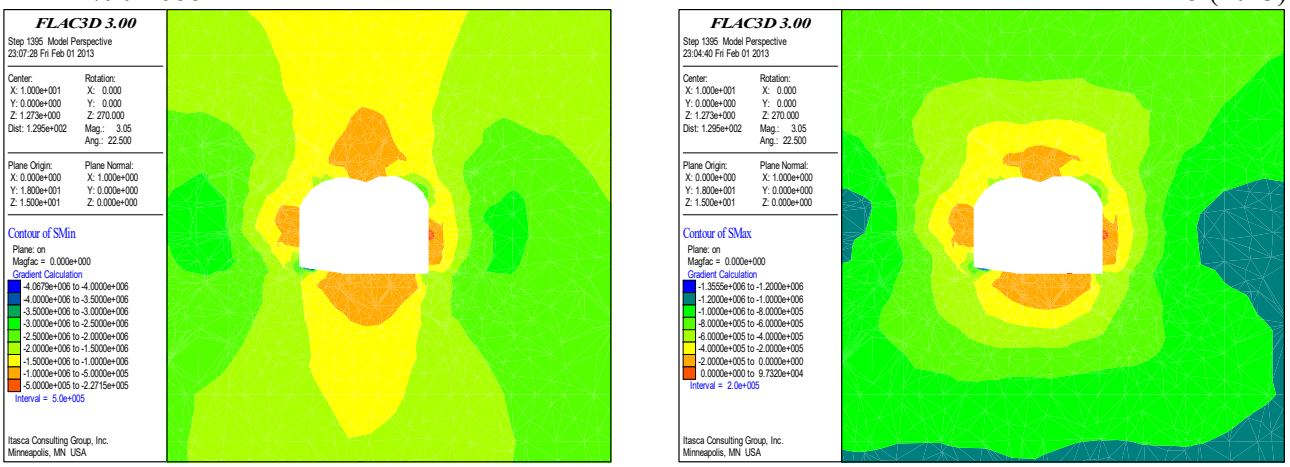


a. Maximum b. Minimum

Fig 6 Section 3-3 principal stress nephogram

### 4.2 Structural stability analysis without support after excavation

Due to the influence of the intersection, the settlement of the linings of the Fuliang branch line 2# tunnel and the construction gallery 12# at the top are both increased. The influence range on the obtuse angle side of the Fuliang branch line 2# tunnel is about 6m, and that on the acute angle side is about 9m, while that of the construction gallery 12# is about 11m. The maximum settlement of the lining is 9.3mm, which occurs at the intersection of the two tunnels on the acute angle side, as shown in Fig 7.

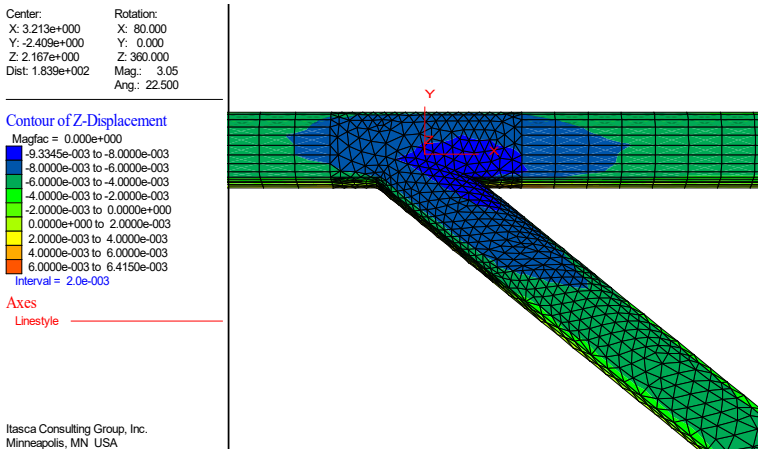


Fig 7 Vertical displacement of the external surface of the top lining

Section 1-1 is located in the vertical plane along the axis of the Fuliang branch line 2# tunnel. The vertical displacement of the section along the axis of the Fuliang branch line 2# tunnel increases near the intersection of the two tunnels, and the settlement of the top of the arch frame at a distance from the intersection is about 5mm (↓), which is 1mm smaller than that without support, and the uplift of the bottom slab is about 4mm (↑), which is 1mm smaller than that without support. At the intersection of the two tunnels, the maximum settlement of the top of the arch frameis 8.2mm (↑), which is 1.4mm smaller than that without support, and the maximum uplift of the bottom slab is 6.5mm (↓), which is 1.2mm smaller than that without support, as shown in Fig 8(a).

Section 2-2 is located in the vertical plane along the axis of the construction gallery 12#. The maximum values of the settlement of the arch crown and the uplift of the bottom slab of the construction gallery 12# occur at the intersection with the Fuliang branch line 2#, with the maximum value of the settlement of the arch crown being 9.3mm (↓), which is 1.5mm smaller than that without support, and the maximum value of the bottom slab uplift being 6.5mm (↑), which is 1.1mm smaller than that without support. The deformation of the surrounding rock within 14m from the intersection point of the construction gallery 12# is greatly affected by the intersection. See Fig 8(b).

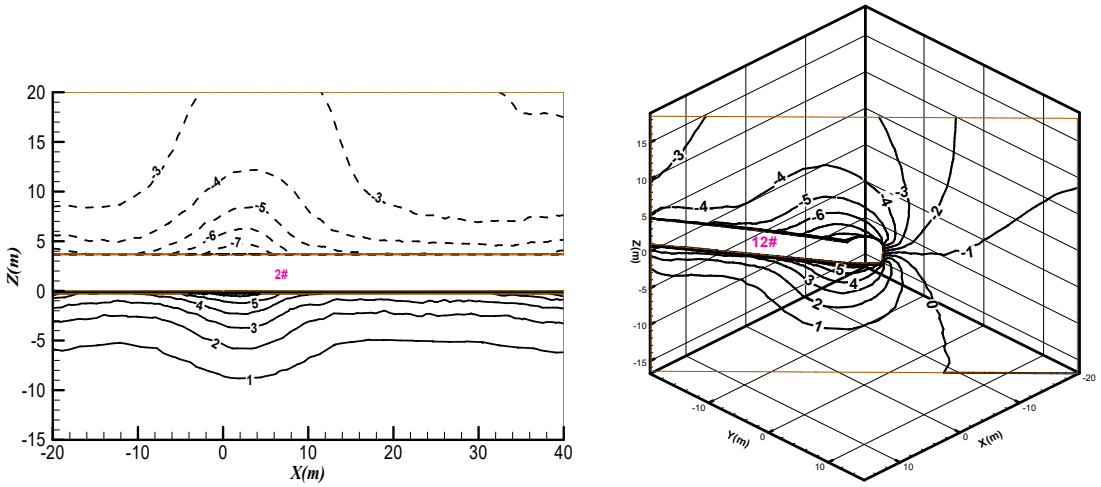


a Section 1-1 b.Section 2-2

Fig 8 Vertical displacement contour

Section 3-3 is located at the x=0m position where the axes of the two tunnels intersect and is perpendicular to the axis of the Fuliang branch line 2# tunnel. The maximum settlement is 8.7mm (↓), which occurs at the intersection of the two tunnel linings at the top and is 1.5mm smaller than that without support, and the maximum uplift of the bottom slab is 6.5mm (↑), which is 1.0mm smaller than that without support, as shown in Fig 9 (a).

The maximum horizontal displacement at the middle of the right sidewall of the Fuliang branch line 2# tunnel is 6.2mm, which is 1.3mm smaller than that without support, and the maximum horizontal displacement at the middle of the left sidewall of the construction gallery 12# is 4.8mm, which is 1.9mm smaller than that without support. See Fig 9 (b).

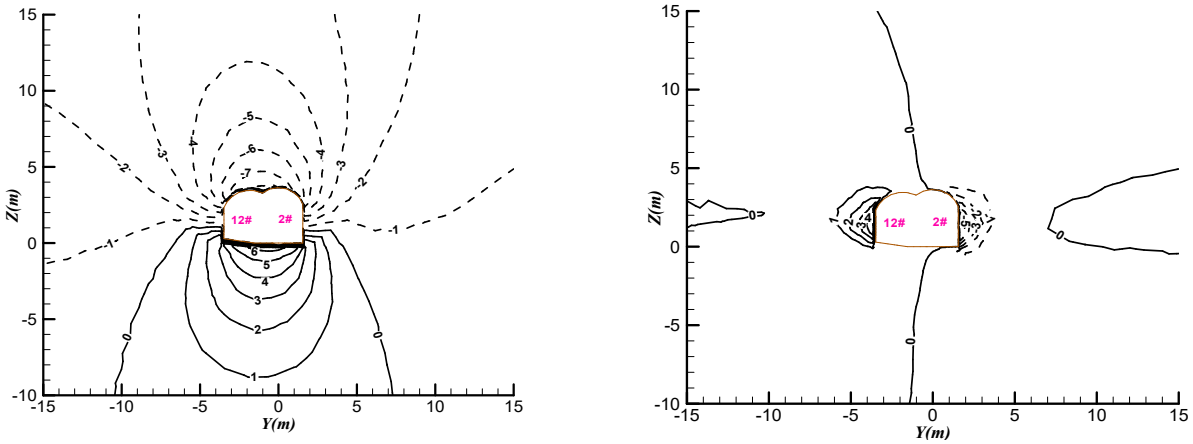


a.Vertical b.Horizontal

Fig 9 Section 3-3 vertical and horizontal displacement contours

The maximum compressive stress is 2.68 MPa, located at the bottom of the left sidewall of the construction gallery 12#, which is 1.39 MPa smaller than 4.07 MPa without support; the compressive stress of the right arch waist of the 2# branch tunnel is reduced from 3.0 MPa without support to 2.2 MPa, which is reduced by 0.8 MPa; the maximum principal stress is shown in Fig 10 (a).

The right sidewall of the Fuliang branch line 2# tunnel does not appear in the tension zone again, but the intersection of the top linings of the two tunnels appears in the tension zone, with the maximum tensile stress being 0.73 MPa. At the sharp corner where the two linings intersect, the rock block is unstable. Under the action of the weight of the sprayed concrete, the rock mass at the sharp corner is in a tension state. See Fig 10 (b). It is recommended in actual construction that the linings shall be smoothly intersected and the steel arch frame shall be used to provide early support force in time, and cross anchor bars shall be bored in advance if necessary.

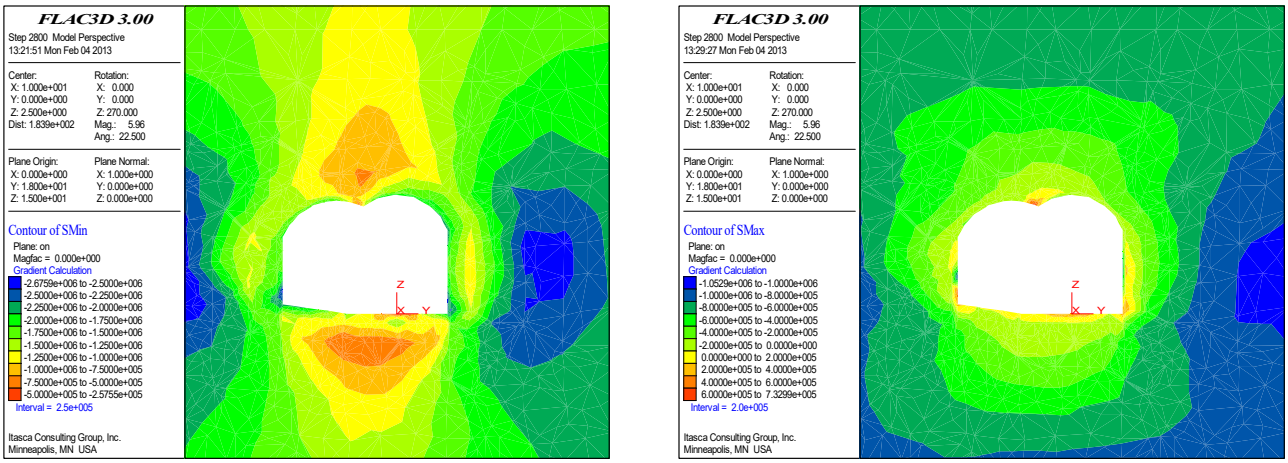


a. Maximum b. Minimum

Fig 10 Section 3-3 principal stress nephogram

## Conclusion

I(1) The steel arch support can provide rapid radial pressure to the surrounding rock of the cavern and effectively improve the self-supporting capacity of the surrounding rock, quickly inhibit the continued relaxation and plastic zone of the surrounding rock, and controls the initial deformation of the cavern and the range of the plastic zone of the surrounding rock. Make the displacement of the surrounding rock greatly reduced, and the stability of the initial support is improved significantly. (2) Before the steel arch support is added, the displacement of each calculated section of the cavern intersection is relatively large, and the shallow surface of the local position of the intersection tunnel of the intersection section occurs plastic failure or partial collapse. Therefore, for such a surrounding rock cavern, rigid support should be carried out. (3) The cavern is supported by the combined support of "arch frame + net hanging + anchor rod + shotcrete". After support, the deformation and displacement of the characteristic points of each calculated section are smaller than those without support. This type of support can play a certain role in restraining the deformation and displacement of the surrounding rock in the intersection section. (4) At the intersection of the two tunnels, the arching effect of the lining is destroyed, and the stress concentration effect of the surrounding rock occurs at the intersection. Therefore, the obvious increase in the range of displacement occurs in the range of about 10m on the obtuse side and about 16m on the acute side of the intersection of the 2# branch tunnel, and in the range of 14m of the 12# construction access. (5) In the combined support, the steel arch frame, shotcrete, and reinforcement net deform together and bear part of the rock pressure respectively. While the concrete strength increases, the pressure on the steel arch frame at the initial stage shifts to the support concrete layer. The plastic deformation pressure and rheological pressure in the later stage are mainly borne by the concrete layer and the steel arch frame, and the main role of the reinforcement net is to prevent the concrete spray layer from cracking.

## Reference

[1] Zhang X J,etc. Study on construction technology of intersection section between inclined shaft and main tunnel of water-conveying tunnel with large slope[J]. Tunnel Construction(Chinese and English),2023,43(S1):382-390.

[2] Meng G L,etc. Blasting construction scheme design of intersection section of new water-conveying tunnel[J]. Engineering Technology Research,2023,8(13):61-63.

[3] Liu K W,etc. Numerical simulation analysis of surrounding rock stability of water-conveying tunnel[J]. Shanxi Water Conservancy,2022(10):134-135.

[4] Guo J T. Study on the influence of embedment depth on the safety of construction of shallow-embedded water-conveying tunnels[J]. Jilin Water Conservancy,2022(09):38-41.

[5] Mao X C. Failure characteristics analysis of lining structure of water-conveying tunnel based on numerical simulation[J]. Hydraulic Science and Cold Region Engineering,2023,6(08):41-44.

[6] Ma F,etc. Numerical simulation analysis of TBM construction in deep super-long water-conveying tunnel of Middle Route of Yellow River Diversion Project[J]. Water Conservancy Construction and Management,2022,42(08):1-7+26.

[7] Zhang H. Study on mechanical effect and deformation mechanism of rock mass unloading in tunnel[D]. Chongqing Jiaotong University,2015.

[8] Kang Y M.Numerical simulation of stress change law of surrounding rock during construction of double tunnels in high stress area[J]. Energy and Environmental Protection,2022,44(06):272-278.

[9] Zhou Yabo, etc. Study on rock-support interaction and support timing in deep fractured roadway[J]. Metal Mine, 2022(06): 17-23.

[10] Zhang Yuxian, etc. Study on construction process simulation system of water diversion tunnel considering rock stability evaluation[J]. Water Resources and Power, 2020, 38(09): 109-113.

[11] Liu Kuan. Study on the stability of surrounding rock in the intersection section of tunnels and treatment measures of existing tunnels[D]. Huazhong University of Science and Technology, 2020.

[12] Zhou Feng, etc. Study on the long-term stability of the intersection section of Zouma tunnel and water supply tunnel[J]. Chinese Journal of Underground Space and Engineering, 2018, 14(S2): 913-918.